Electronic Supplementary Material (ESI) for Journal of Materials Chemistry A.

Supporting Information

Tri-layered Graphite Foil for Electrochemical Capacitors

Yu Song, Tian-YuLiu, Guo-Liang Xu, Dong-Yang Feng, Bin Yao, Tian-YiKou, Xiao-Xia Liu and Yat Li**

Y. Song, G. -L. Xu, D. -Y. Feng, Prof. X. -X. Liu
Department of Chemistry
Northeastern University
Shenyang 110819, P. R. China
*E-mail: xxliu@mail.neu.edu.cn

Y. Song, T. -Y. Liu, B. Yao, T. -Y. Kou, Prof. Y. Li
Department of Chemistry and Biochemistry
University of California- Santa Cruz
1156 High Street, Santa Cruz, CA 95064, USA
*E-mail: yatli@ucsc.edu

1. Calculations

1.1 Specific capacitance calculation based on constant current charge/discharge experiments

Gravimetric and areal capacitance of a single electrode from the constant current charge-discharge profile are calculated from equation S1 and S2:

$$C_m = \frac{It}{m\Delta U} \qquad \text{(Equation S1)}$$

$$C_a = \frac{It}{S\Delta U} \qquad \text{(Equation S2)}$$

Where C_m and C_a are the gravimetric and areal specific capacitance (Fg^{-1} or $mFcm^{-2}$), S is the electrode area (cm^2), I represents the discharge current (mA), m is the mass of the entire electrode (mg), t is the discharge time (s) and ΔU is the potential window (V).

Gravimetriccapacitance of the ASC device from the constant current charge-discharge profile is calculated from equation S3:

$$C_m = \frac{It}{mU} \qquad \text{(Equation S3)}$$

Where $C_m$is the gravimetric capacitance of the ASC (Fg^{-1}), I represents the discharge current (mA), m is the mass of both electrodes (mg),t is the discharge time (s) and U is the potential window of the ASC (V).

1.2 Energy density and power density calculations for the ASC device

Gravimetric Energy density (E, $Whkg^{-1}$) and power density (P, Wkg^{-1}) are calculated using the following two equations:

$$E_m = \frac{1000}{2 \times 3600} C_m U^2 \qquad \text{(Equation S4)}$$

$$P_m = \frac{3600 \times E_m}{t} \qquad \text{(Equation S5)}$$

Where $C_m$is the specific capacitance (Fg^{-1}), U is the operating voltage (V) and t is the discharge time (s) measured in constant current charge/discharge experiments.

2. Supporting Figures

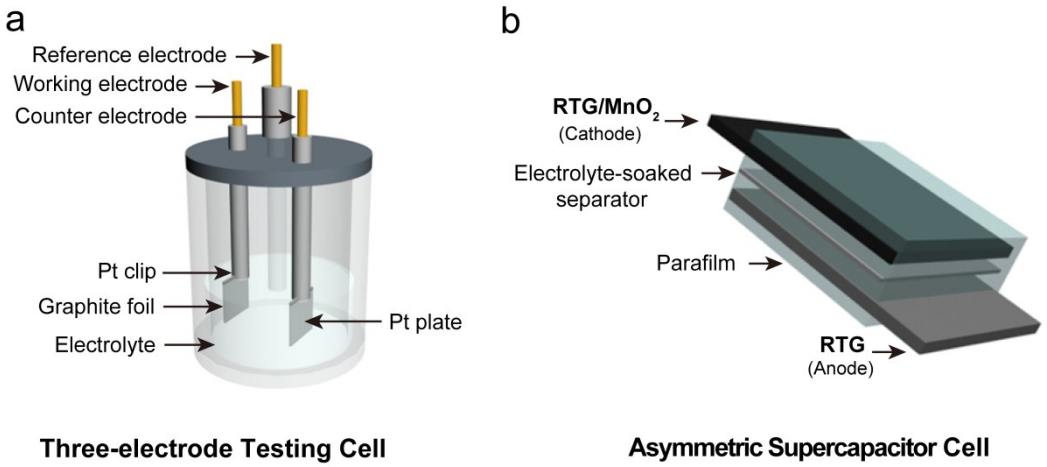

Figure S1. Schematic illustration of (a) the three-electrode cell for electrochemical measurements, and (b) the device architecture of the RTG//RTG/MnO_2 asymmetric supercapacitor.

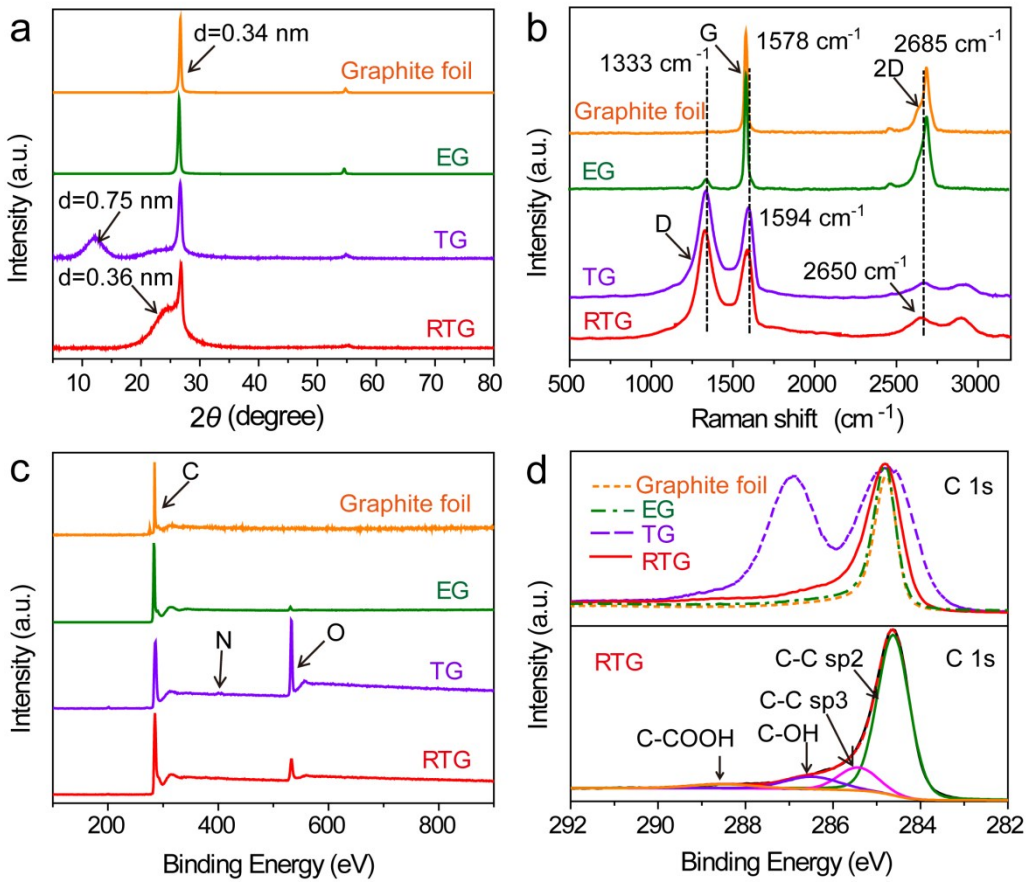

Figure S2. (a) XRD pattern of graphite foil, EG, TG and RTG. (b) Raman spectra of graphite foil, EG, TG and RTG. (c) XPS survey spectra of graphite foil, EG, TG and RTG. (d) XPS core spectra of C 1s for graphite foil, EG, TG and RTG.

In Figure S2b, the slightly increased Raman intensity of D peak in EG should originate from the increased defect sites after the exfoliation. The intensity of the D peak of TG increased considerably, suggesting more defects (such as oxygen functional groups and small graphene domains) were introduced into the original graphitic lattice during the electrochemical intercalation. In addition, the wave number of G peak in TG is slightly higher than that of graphite foil and EG, which can be attributed to the intercalation of NO_3^-.[*Anal. Chem.,* ***1992****, 64, 1528-1533; Nanoscale,* **2015**, 7, 3581-3587] The peak position of G band (corresponds to E_{2g} mode) is sensitive to ion intercalation. Formation of ion intercalated compounds will red shift the G band, due to change in symmetry at the graphite boundary

layer and electronic effects of the intercalated ions. [*Anal. Chem., **1992**, 64, 1528-1533*] There is a blue shift of 2D peak after ion intercalation, indicating the decreased numbers of graphene layers.[*Nanoscale,* **2015**, 7, 3581-3587] These results revealed that the graphite layers were further exfoliated after ion intercalation, leading to enhanced ion accessible surface area, which is consistent with the SEM and TEM results.

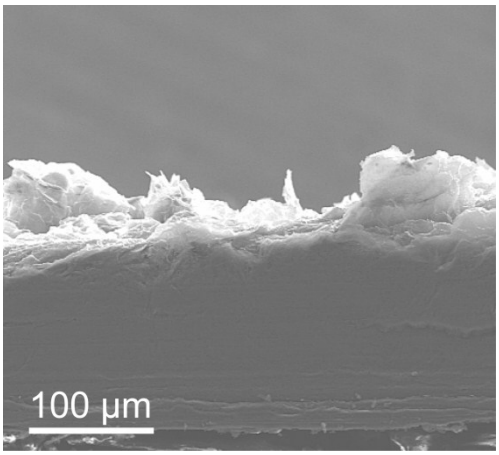

Figure S3. Side view SEM image of EG treated in 0.5 M phosphoric aqueous solution at 1.8 V (vs. SCE) for 3h.

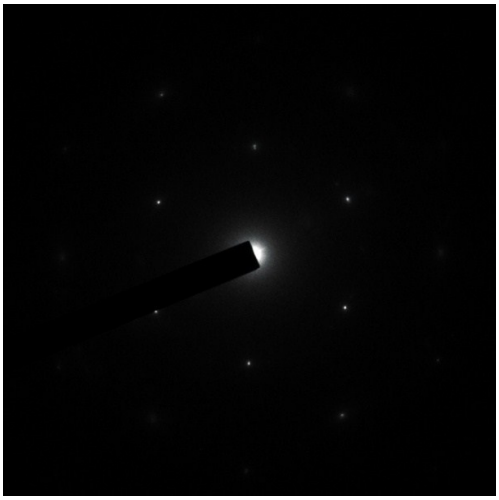

Figure S4. The selected area electron diffraction pattern of exfoliated graphene sheet.

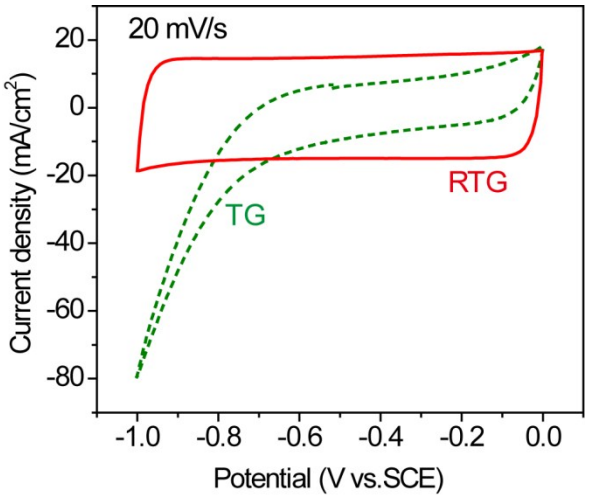

Figure S5. CV curves of TG and RTG collected at 20 mV s^{-1}.

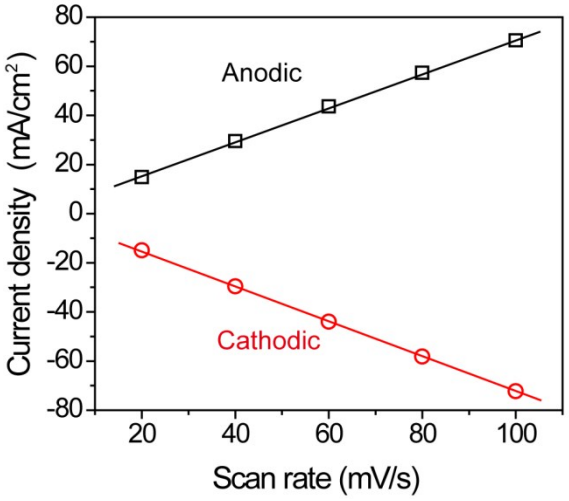

Figure S6. Plot of anodic and cathodic current density of RTG against scan rates.

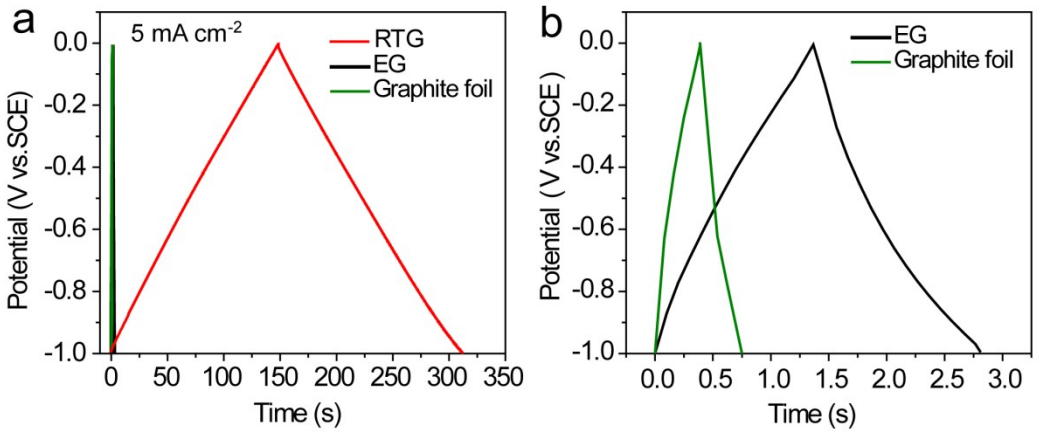

Figure S7. (a) Constant current charge/discharge curves of (a) RTG, EG and untreated graphite foil and (b) EG and untreated graphite foil collected at a current density of 5 mA cm^{-2}.

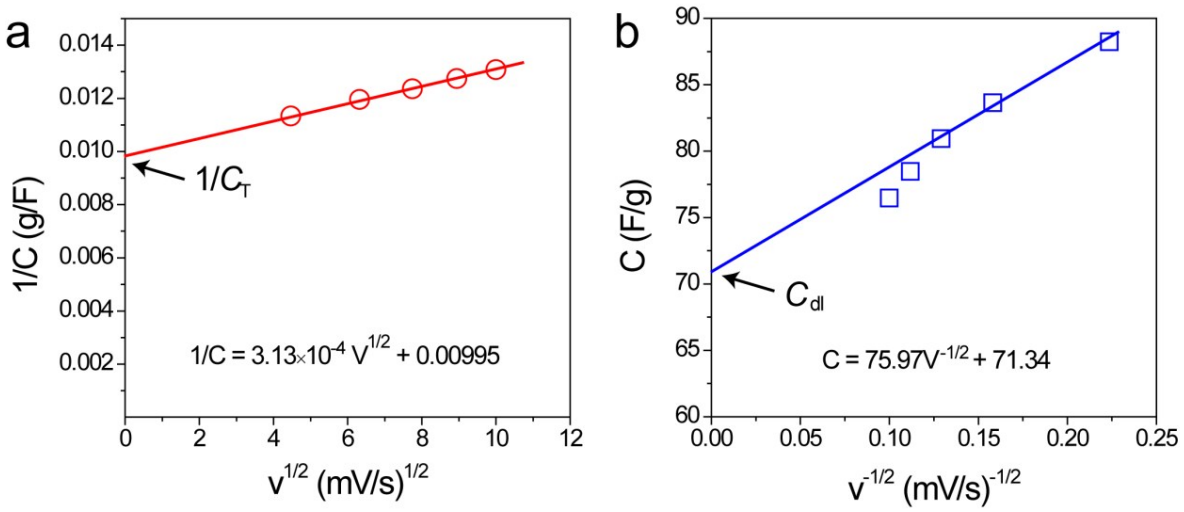

Figure S8. (a) Plot of $1/C$ vs. $v^{1/2}$ and (2) plot of C vs. $v^{-1/2}$. Open circles/squares and solid lines represent the capacitances evaluated using CV curves and the fitting lines, respectively. Gray data points are masked during linear fitting.

First, capacitances were calculated using the corresponding CV curves via the following equation:

$$C = \frac{S}{2 \cdot \Delta U \cdot v}$$

Where C stands for the gravimetric capacitance (in F g^{-1}), ΔU the potential window (in V), S the area enclosed by corresponding cyclic voltammograms (in A V g^{-1}) and v the scan rate (in V s^{-1}). A linear correlation of $1/C$ vs. $v^{1/2}$ is expected assuming ion diffusion follows a semi-infinite diffusion pattern

(Figure R1a). Fitting the data points with a straight line and extrapolating the fitting line to y-axis (*i.e.*, $v \rightarrow 0$) yields the reciprocal of total capacitance ($1/C_T$). C_T represents the highest possible capacitance since when $v \rightarrow 0$, ions in the electrolyte should have enough time to diffuse to all accessible surface area and pseudo-capacitive active sites. C_T is the sum of C_{dl} and C_P.[*J. Power Sources*, **2013**, 227, 300-308]

Similarly, a linear dependence of C vs. $v^{-1/2}$ should also be observed assuming semi-infinite ion diffusion (Figure R1b). However, some data points collected at large scan rates deviate the linear trend due to intrinsic electrical resistance of the electrode.[*ACS Nano*,**2013**, 7, 1200-1214] Therefore, we only fitted the capacitances at slow scan rates. Extrapolating the fitting line to y-intercept (*i.e.*, $v \rightarrow +\infty$) yields the C_{dl} since when $v \rightarrow +\infty$, all capacitance with relatively slow kinetic (*i.e.*, pseudo-capacitance in this case) should be eliminated.[*J. Power Sources*,**2013**, 227, 300-308] Subtracting C_{dl} from C_T gives C_P. The C_T, C_{dl} and C_P of RTG are calculated to be 100.59 F g^{-1}, 71.43 F g^{-1} and 29.16 F g^{-1}, respectively.

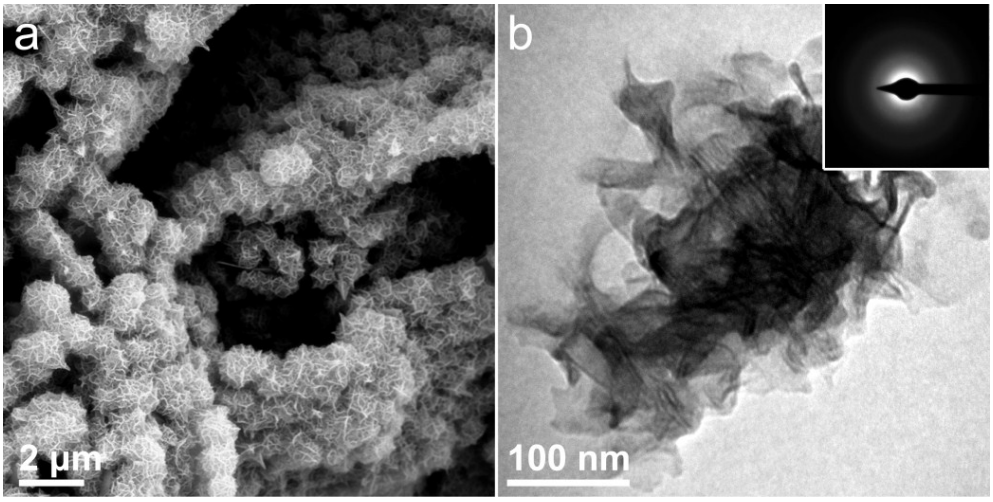

Figure S9. (a) SEM image and (b)TEM image of RTG/MnO_2. Inset shows the selected area electron diffraction (SAED) pattern of detached MnO_2, indicating its amorphous nature.

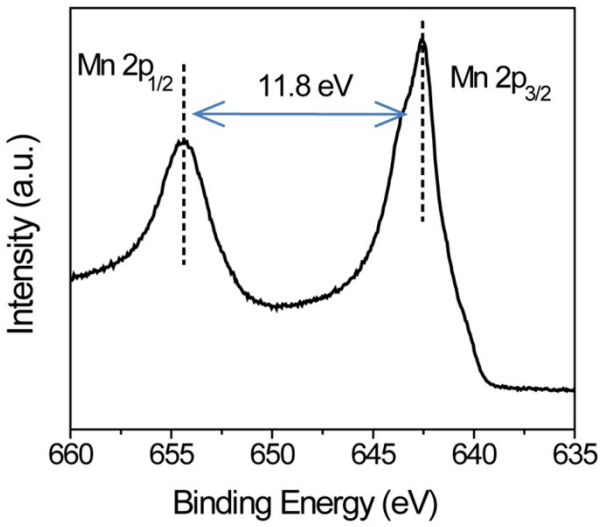

Figure S10. XPS core spectra for Mn 2p.

Two peaks located at *ca.* 654.4 and 642.6 eV are observed with a spin-energy separation of 11.8 eV, which can be ascribed to the Mn $2p_{1/2}$ and Mn $2p_{3/2}$ spin-orbit peaks of MnO_2, respectively.[*Nanoscale,* **2015**, 7, 3581-3587]

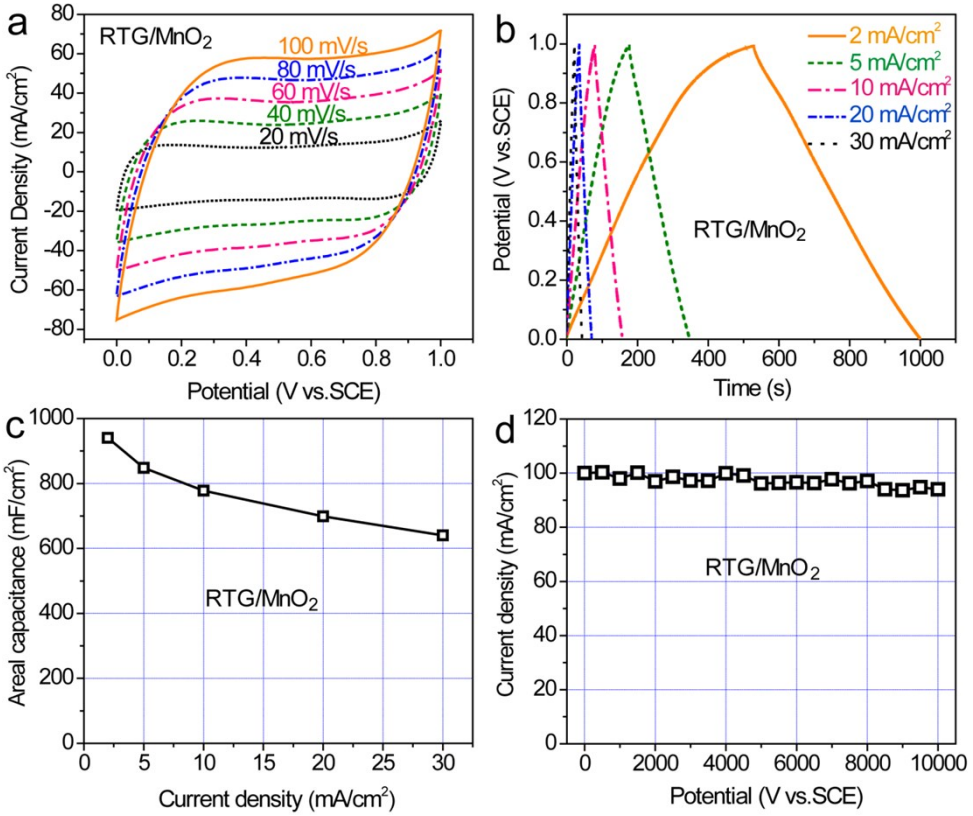

Figure S11. Electrochemical performance of RTG/MnO_2. (a) CV curves of RTG/MnO_2 collected at different scan rates. (b) Constant current charge/discharge curves of RTG/MnO_2 collected from 2 to 30 mA/cm^2. (c) Areal capacitance of the electrode as a function of current densities. (d) Cycling stability of RTG/MnO_2 at current density of 30 mA cm^{-2} for 10000 cycles.

To investigate electrochemical properties of the electrode, RTG/MnO_2 was cyclic voltammetric scanned from 20 to 100 mV s^{-1} in 3M KCl aqueous electrolyte with a three-electrode configuration, using a graphite foil as counter electrode and SCE as reference electrode **(**Figure S11a). It can be seen that all of the CV curves exhibit approximately rectangular shapes, which indicates the ideal capacitive behavior of the sample. In agreement with the CV results, the galvanostatic charge/discharge curves of the the sample show good symmetry and fairly linear slopes between 0 and 1 V from 2 to 30 mA cm^{-2}, indicating fast and reversible Faradic reactions of MnO_2 nanosheets, with electrolyte cations (K^+ or H^+) involved (Figure S11b). The areal capacitance of RTG/MnO_2 calculated from galvanostatic charge/discharge

curves obtained at 2 mA cm^{-2} was 940 mF cm^{-2}. REG/MnO_2 also exhibited good rate capability with 70% capacitance retention when the current densities was increased to 30 mA cm^{-2} (Figure S11c). In addition, RTG/MnO_2 showed good cycling stability and 94% capacitance retention could be maintained after 10000 cycles (Figure S11d).

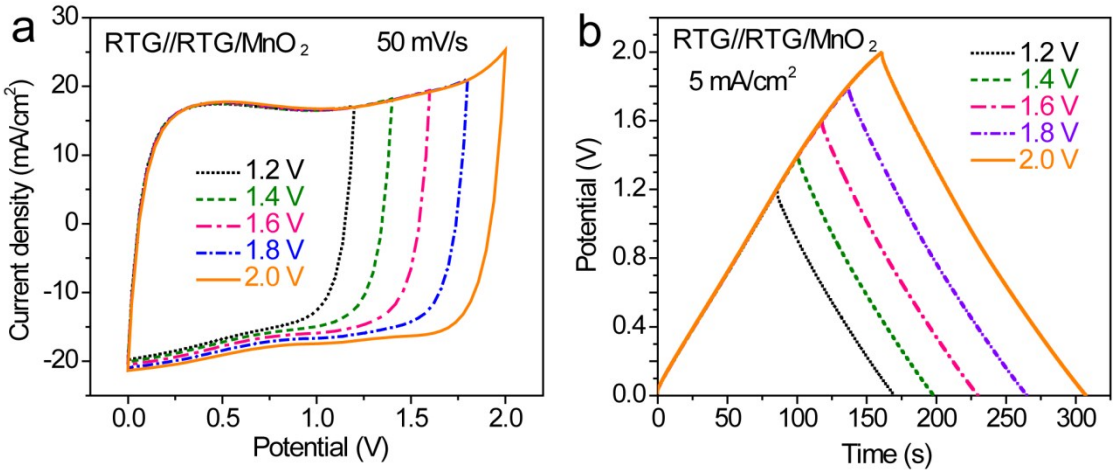

Figure S12. CV and constant current charge/discharge profile of the ASC.

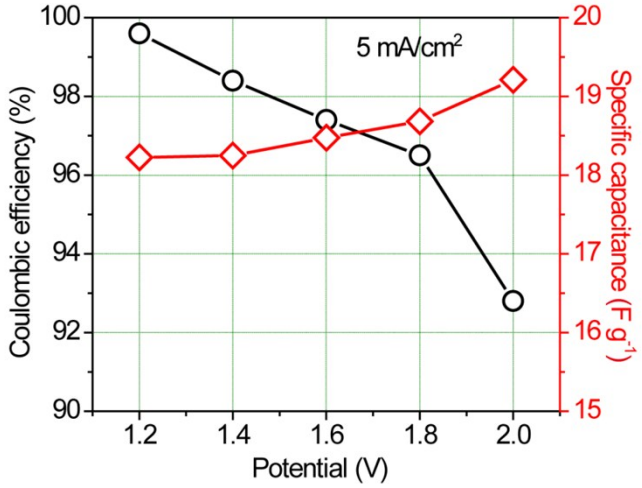

Figure S13. Plots of specific capacitance and coulombic efficiency of the ASC device, collected at the current density of 5 mA cm^{-2}, as a function of potential window.